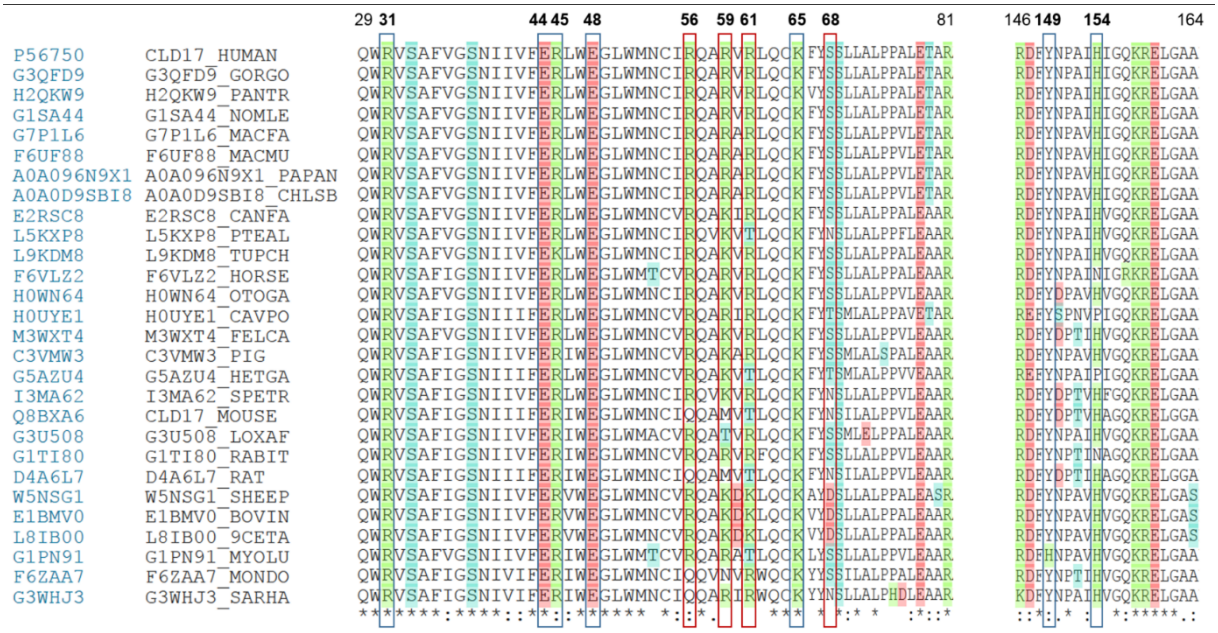

Figure S1. Multiple sequence alignment of ECL1 (left) and ECL2 (right) for Cldn17. 28 orthologous sequences available in UNIPROTKB were aligned using CLUSTAL O (McWilliam et al., Nucleic Acids Res. 2013 Jul; 41(Web Server issue: W597-600.)). Accession number and species is given on the left; residue number is given on top; green, positively charged; red negatively charged; cyan Ser/Thr; *, identical; :, strongly similar properties;., weakly similar properties. The sequences are shown with positions 29 - 81 and 146-164 (ECL1 and ECL2 as defined by uniprot.org). Boxes mark the residues analyzed in this study. Blue boxes mark positions with identical or highly similar residues whereas red boxes mark positions with residues containing different properties (TIFF 2337 kb)

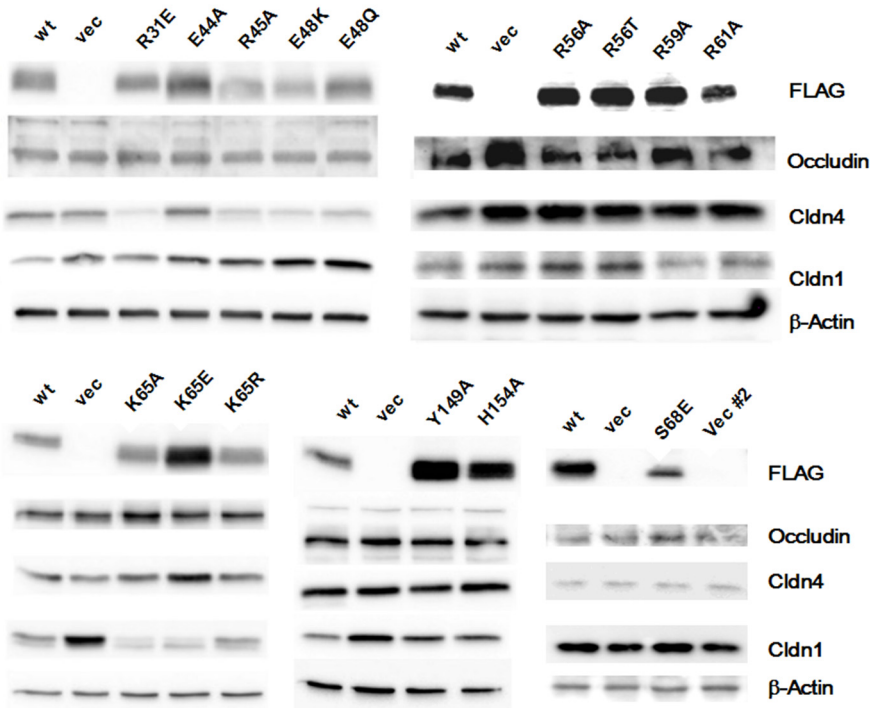

Figure S2. Exemplary western blots for other TJ proteins. The blots show exemplary clones of each mutation in comparison to wt Cldn17 and vector control (vec). Detected were Cldn1, Cldn4, occludin, the FLAG-tagged Cldn17 and β-actin as loading control. Expression changes occurred in some, but not all, clones of one mutant. However, these changes had no impact on functional results, as these were similar in all clones of one mutant (TIFF 221 kb)

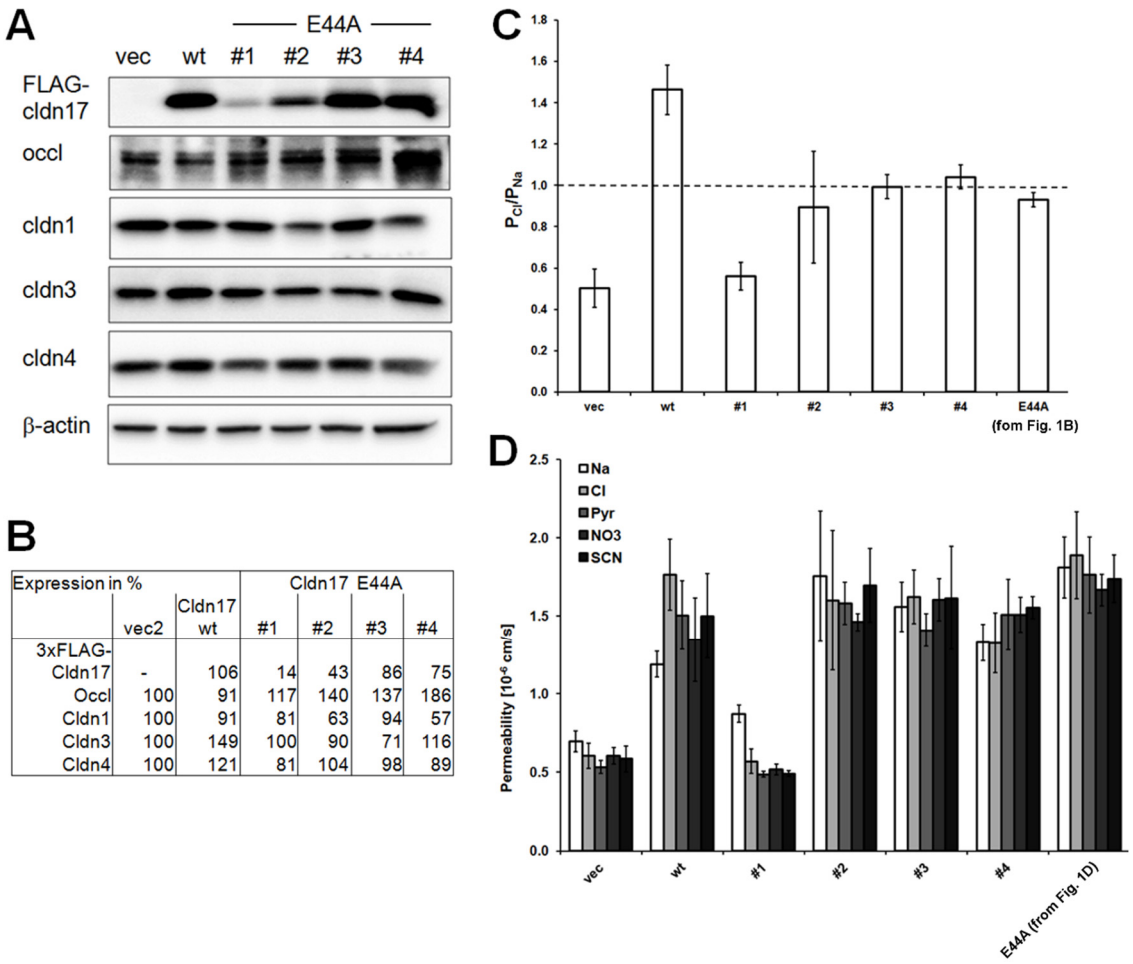

Expression in %			Cldn17 E44A			
	vec2	Cldn17 wt	#1	#2	#3	#4
3xFLAG-Cldn17	-	106	14	43	86	75
Occl	100	91	117	140	137	186
Cldn1	100	91	81	63	94	57
Cldn3	100	149	100	90	71	116
Cldn4	100	121	81	104	98	89

Figure S3. Exemplary comparison of different clones (E44A). **a** The blots show exemplary clones of mutation E44A in comparison to wt Cldn17 and a vector control (vec). Detected were Cldn1, Cldn4, occludin, the FLAG-tagged Cldn17 and β-actin as loading control. **b** The densitometric analysis revealed expression differences which may influence the results of further experiments. However, only a very low mutant expression of 14 % (clone #1) compared to the wt, resulted in P_{Cl}/P_{Na} as observed for the vec, while ranges of expression above 43 % to 86 % were comparable to each other **c**. Also permeabilities for other ions **d** were only different from the other clones at very low expression levels. Additional expression variations in endogenous TJ protein levels had no effect in the ranges observed. However, to keep clonal variation as low as possible, several clones were analyzed for each mutant and outliers with extreme differences in expressions were excluded (TIFF 3315 kb)

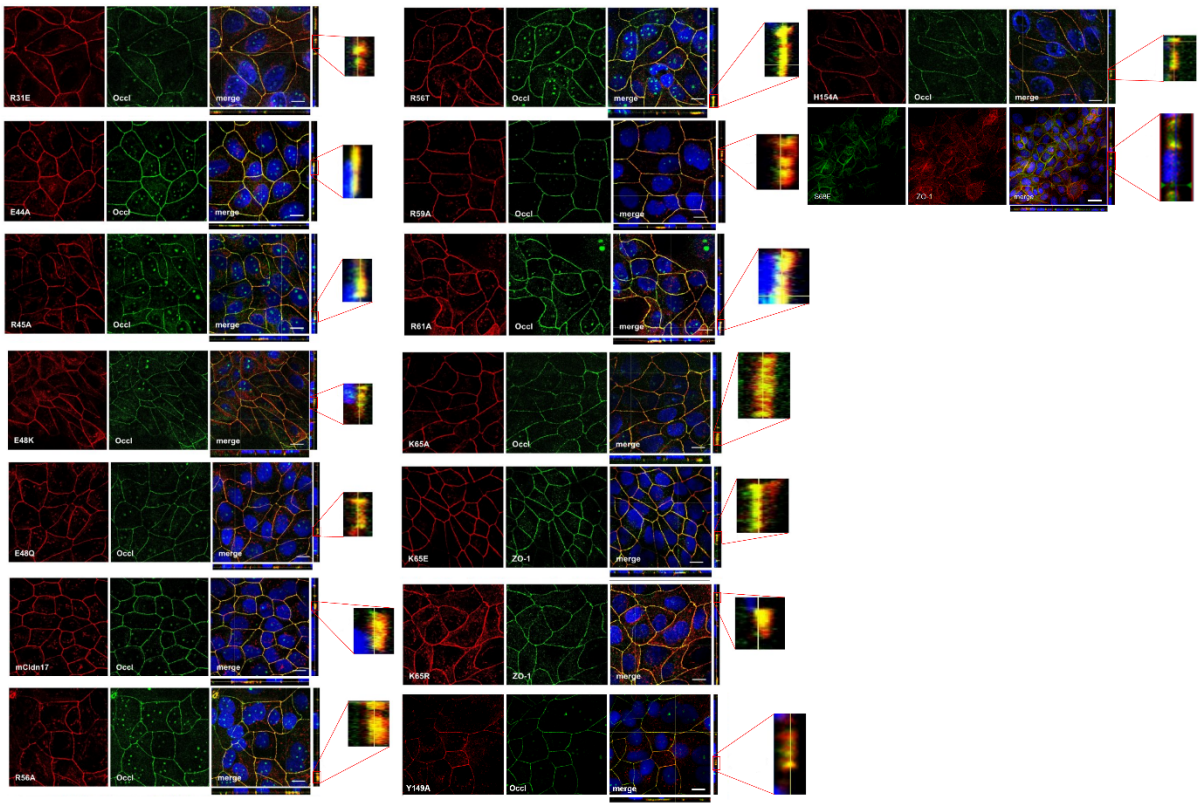

Figure S4. Immunofluorescent staining of exemplary clones. Localization of the 3 × FLAG-tagged mutants of Cldn17 (red) was analyzed using occludin or ZO-1 (green) as TJ marker. All mutant Cldn17 constructs were colocalized (yellow) with the TJ marker, indicating correct insertion into the TJ. Bar = 10 µm (TIFF 16234 kb)

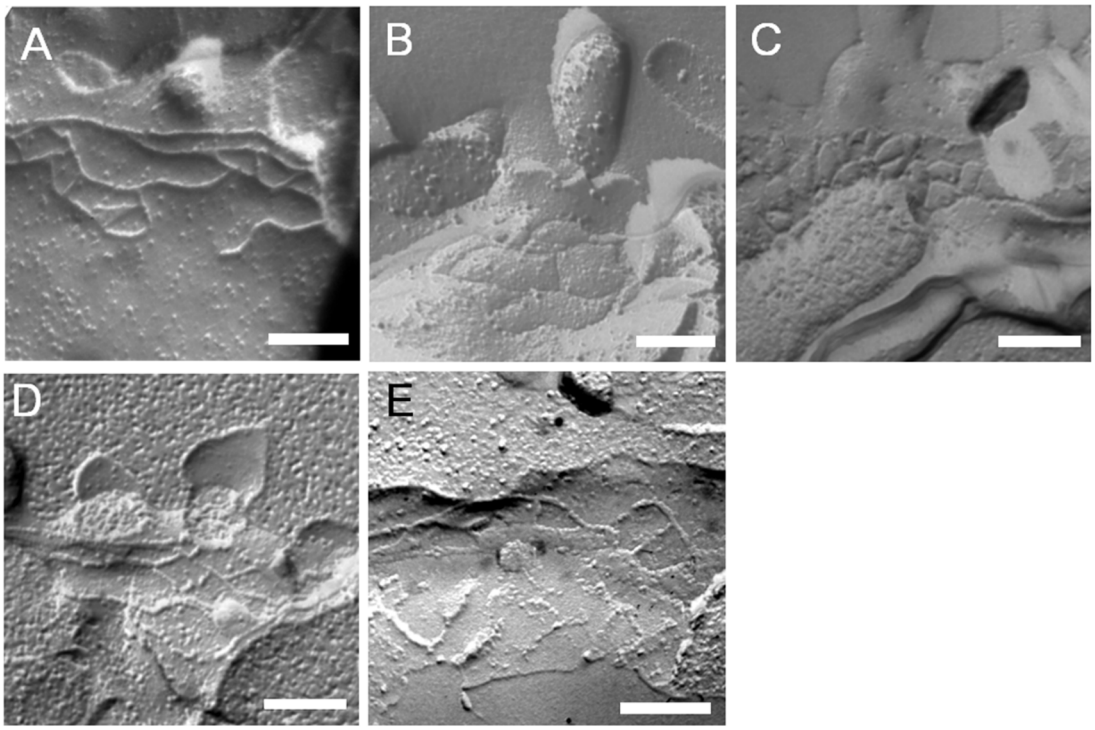

Figure S5. Exemplary images of freeze-fracture electron microscopic samples. Mutation from anion- to cation-selective Cldn17 (mutant K65E) as well as the other mutations of K65 that led to loss of charge selectivity had no effect on TJ ultrastructure. **a** Vector-transfected control. **b** wt Cldn17. **c** Cldn17 K65E. **d** Cldn17 K65A. **e** Cldn17 K65R. Bar = 200 nm (TIFF 4714 kb)

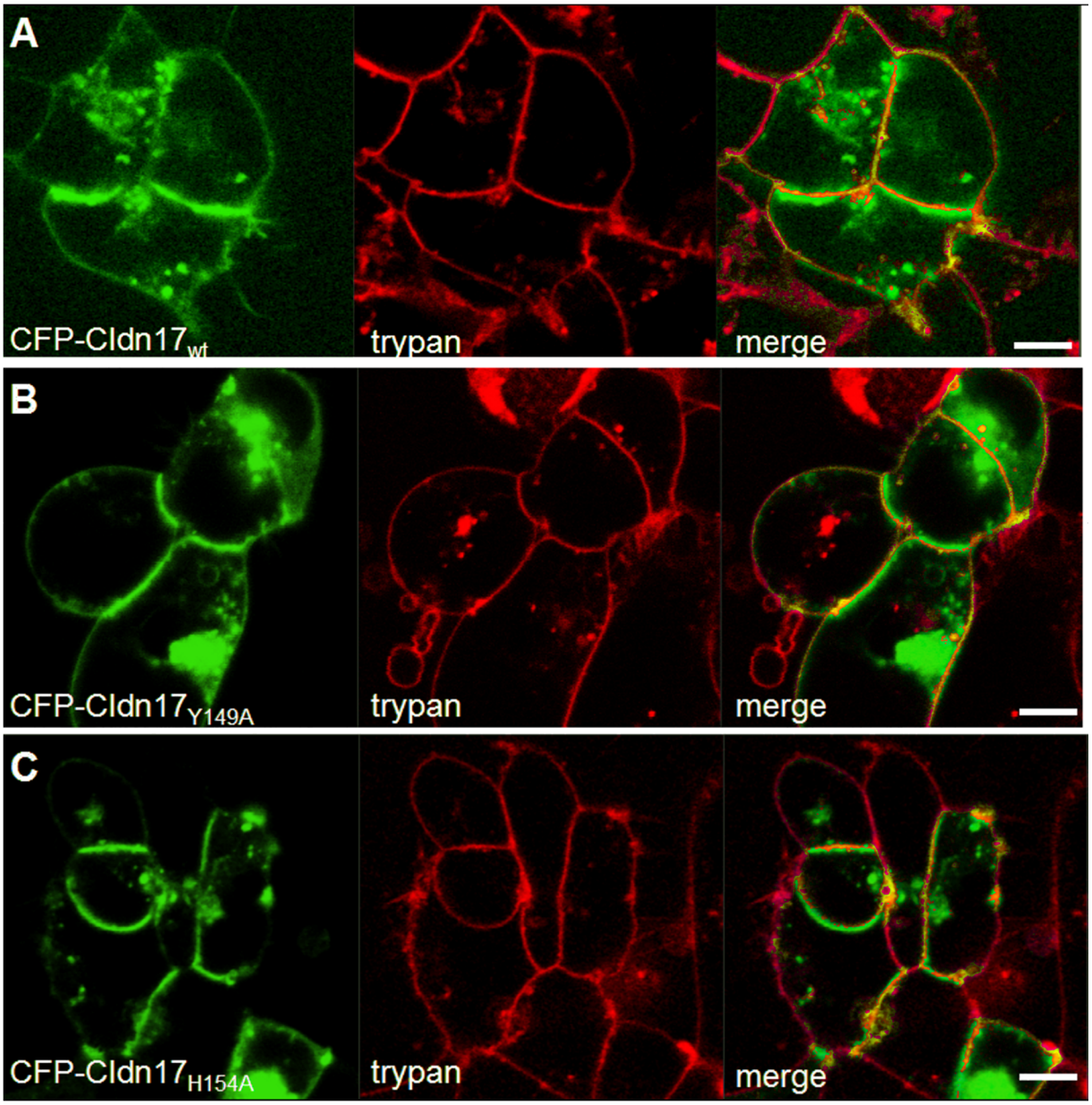

Figure S6. Live cell imaging of HEK293 cells transfected with three CFP-tagged constructs. Subcellular localization of **a** wtCldn17, **b** Cldn17 Y149A and **c** Cldn17 H154A (green). Trypan blue (red) marks the cell membrane. All three Cldn17 constructs were expressed and localized within the cell membrane. Enrichment in cell membranes of neighboring cells indicates the ability to *trans*-interact. Bar 5 µm (TIFF 20632 kb)

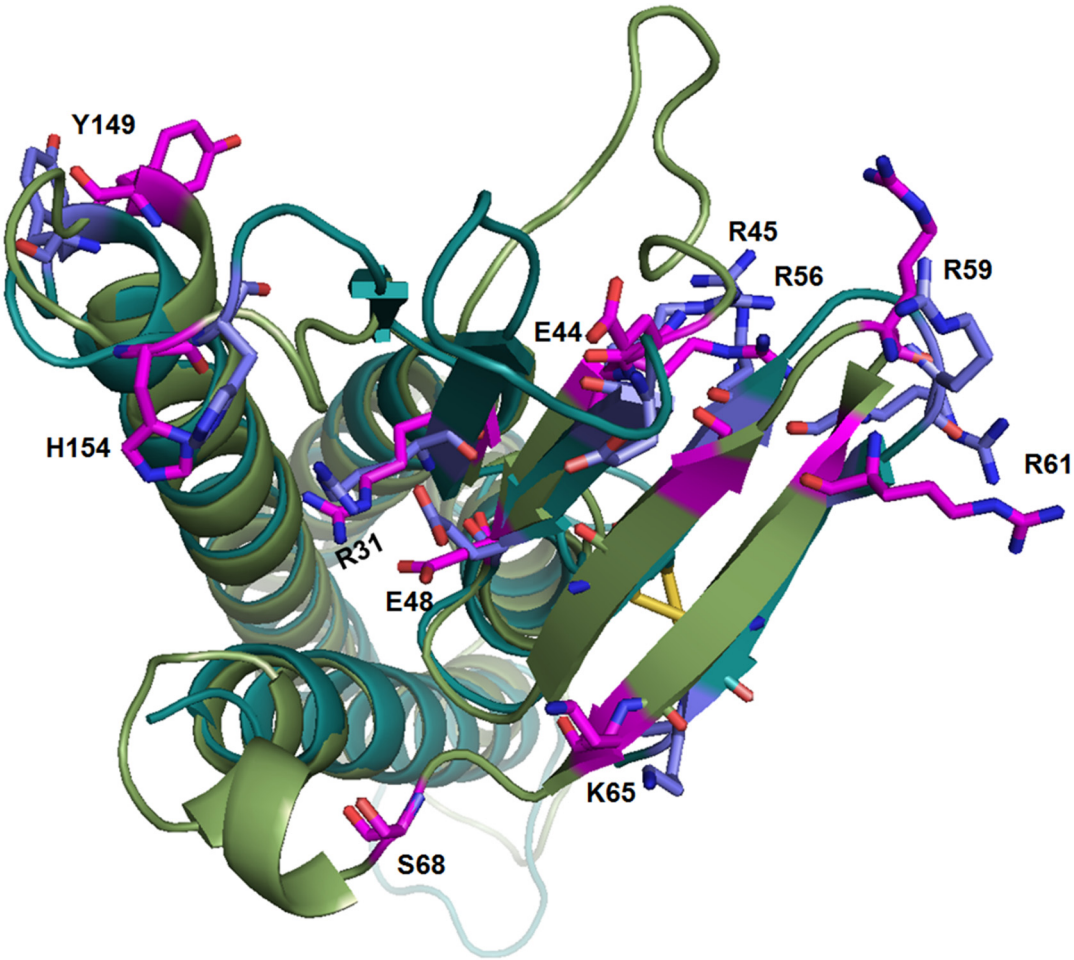

Figure S7. Overlay of Cldn17 and Cldn19 homology models. Comparison of Cldn17 homology models based on templates for Cldn15 (PDB: 4P79, backbone as cartoon in green, residues as sticks in magenta) and Cldn19 (PDB: 3X29, backbone as cartoon in cyan, residues as sticks in violet). Both models indicate a similar fold of Cldn17 and similar positions of the residues (sticks) mutated in this study. However, the models differ in the C-terminal half of ECL2, the loop between β1- and β2-strand and the region between β4-strand and TM2. The latter region was not resolved in the Cldn19 crystal, in which Cldn19 was in complex with the C-terminal domain of the *Clostridium perfringens* enterotoxin [20]. Disulfide bridges in ECL1 are shown as yellow sticks (TIFF 2927 kb)